

Indefinitely flat rotation curves from Mpc sized charged cocoons

THEODORUS MARIA NIEUWENHUIZEN

Institute for Theoretical Physics, Science Park 904, 1098 XH Amsterdam, The Netherlands

PACS 98.62.Dm – Kinematics, dynamics, and rotation

PACS 95.35.+d – Dark matter

PACS 04.20.Jb – Exact solutions

Abstract – Weak lensing exhibits that rotation curves of isolated galaxies remain flat up to Mpc scale (Mistele et al, 2024). Recently we proposed that dark matter is a combination of electrostatic and vacuum energy in standard physics. In this theory, isolated galaxies may be embedded in “charged cocoons”, spheres with $\pm 1/r^2$ charge density. The related circular rotation curves decay at the Mpc scale. The analytic solution is extended to the early Universe. A peak in the cosmic microwave background spectrum is expected at the arcsec scale. The induced nanometer size of the cocoons at the Big Bang makes the initial state inhomogeneous.

arXiv:2411.18221v1 [physics.gen-ph] 27 Nov 2024

Introduction. – Dark matter (DM), established by Zwicky in 1933 [1], causes the flattening of rotation curves for stars and hydrogen clouds. This was evidenced by Rubin and Ford [2] up to some 25 kpc for Andromeda (M31) and out to $122 (0.5/h) = 87 (0.7/h)$ kpc in [3]. Astonishingly, a 2024 analysis of weak lensing by isolated, early and late type galaxies exhibits “indefinitely flat circular velocities”, ranging out to several hundreds kpc, without clear decline out to 1 Mpc [4], the size of a fat galaxy cluster.

This scale of dark matter clouds is difficult to understand within the standard cosmological model Λ CDM [4], with its NFW density profile decaying as $1/r^3$ [5]. It does support MOND [6, 7] and MOND-like theories, see, e. g., [8, 9], where, effectively, the Newton force decays as $1/r$. However, analysis of wide binaries rules out the simplest of those models at 16σ , so that MOND must be substantially modified on small scales [10] (but see [11] for criticism). This adds to tensions of MOND in clusters [12, 13], the solar system [14] and otherwise [7], which motivates to investigate different starting points.

Recently, our analysis of regular black hole interiors [15], the nature of dark matter [16] and the interior of the Lorentz electron [17] have led to assume that, within the standard model of particle physics and classical Einstein-Maxwell theory, the vacuum has a richer structure than commonly considered. It is a state without matter the energy of which can flow and condense with the help of electric fields, so as to establish electro-vacuum energy (EVE) (or “electro-aether energy”, EAE [16]), as the dark mat-

ter. This is supported by the no-show of a dark matter particle in decades of intensive search; by early structure formation triggered by thunders after lightnings due to charge mismatches, and various further aspects [16].

The charged cocoon. – Here we investigate whether in EVE/EAE theory, the indefinitely flat circular rotation curves can be connected to charged spheres, to be called “charged cocoons” (ccs). Consider a spherically symmetric configuration of radius R with charge density $\rho_q(r)$, included charge $Q(r) = 4\pi \int_0^r du u^2 \rho_q(u)$ and total charge $Q(R) = q$. In units $\hbar = c = k = 1$ and $\mu_0 = 1/\epsilon_0 = 4\pi$, the electric field reads $E(r) = Q(r)/r^2$ and the electrostatic energy density $\rho_E = E^2/8\pi$. Neglecting for simplicity the contribution of normal matter, the cc involves electrostatic energy M_E , vacuum energy $M_v = M_E/3$ and total mass $M = 4M_E/3$ for any charge configuration [16].

In the interior (“in”, $r \leq R$), we consider

$$\rho_q^{\text{in}} = \frac{q}{4\pi R r^2}, \quad Q(r) = q \frac{r}{R}, \quad E(r) = \frac{Q(r)}{r^2} = \frac{q}{Rr}. \quad (1)$$

This leads to inverse power laws of the energy densities

$$\rho_E^{\text{in}} \equiv \frac{E^2}{8\pi} = \frac{q^2}{8\pi R^2 r^2}, \quad \rho_v^{\text{in}} = \frac{q^2}{8\pi R^2} \left(\frac{1}{r^2} - \frac{1}{R^2} \right). \quad (2)$$

with $\rho_v = \rho_E^> - \rho_E$ involving $\rho_E^> = 4 \int_r^\infty du \rho_E(u)/u$ [16]. In the exterior (“ex”, $r > R$), $Q(r)=q$, $E=q/r^2$, one has the standard absence of charge and vacuum energy,

$$\rho_q^{\text{ex}} = \rho_v^{\text{ex}} = 0, \quad \rho_E^{\text{ex}} = \frac{q^2}{8\pi r^4}. \quad (3)$$

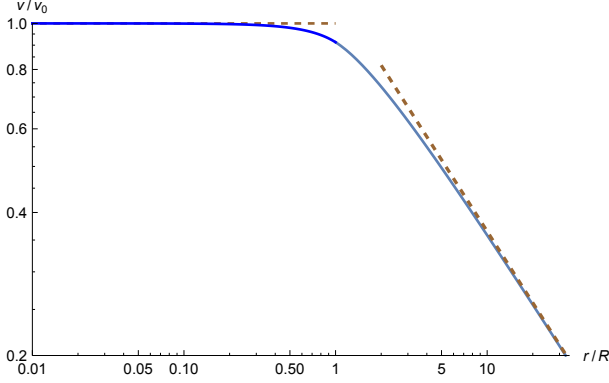


Fig. 1: The “indefinitely flat” profile (6) of rotation curves decays beyond R in line with Newton’s law $v \sim 1/\sqrt{r}$.

The combination $\rho_E + \rho_v = \rho_E^>$ represents the EVE/EAE dark matter density. The included dark mass is

$$M(r) = \begin{cases} (q^2 r/R^2)(1 - r^2/6R^2), & (r < R), \\ (4q^2/3R)(1 - 3R/8r), & (r > R). \end{cases} \quad (4)$$

The full masses of the components follow as

$$M_E = \frac{q^2}{R}, \quad M_v = \frac{q^2}{3R}, \quad M = \frac{4q^2}{3R}. \quad (5)$$

The factor $4/3$ is known from the “problem $4/3$ ”, the ratio of kinematic and electrostatic mass of the Lorentz electron, solved by Poincaré in 1905 for charged spherical shells [18, 19]. His incorporation of the vacuum is the essential piece of our more general electro-vacuum theory [15–17].

Again disregarding the normal matter, the circular rotation speed $v_{\text{rot}}(r) = \sqrt{GM(r)/r}$ attains the profile

$$v_{\text{rot}} = \begin{cases} v_0 \sqrt{1 - r^2/6R^2}, & (r < R), \\ v_0 \sqrt{4R/3r - R^2/2r^2}, & (r > R), \end{cases} \quad (6)$$

which, holding away from the center, involves

$$v_0 = q \frac{\sqrt{G}}{R}, \quad q = v_0 \frac{R}{\sqrt{G}}. \quad (7)$$

The profile (6) is depicted in figure 1.

Physical scales. Consider, for some $\alpha \ll 1$, a number density $n_{\text{cc}} \equiv 3\alpha/4\pi R^3$ of charged cocoons of typical radius R . This involves their average mass density

$$\bar{\rho}_{\text{cc}} = n_{\text{cc}} M = \frac{4\alpha q^2}{3R^4}. \quad (8)$$

Assume that this constitutes a fraction $\alpha\beta^2$ of the critical mass density $\rho_c = 3H_0^2/8\pi G$, with $\beta \approx 2$. This fixes R to the rotation speeds,

$$R = \sqrt{\frac{8}{3}} \frac{v_0}{\beta H_0} = 2.3 v_{200} \text{ Mpc}, \quad (9)$$

where $v_{200} = v_0/(200 \text{ km/s})$ and we take $H_0 = 70 \text{ km/s Mpc}$. Notice that R lies in the Mpc range. The charge is

$$q = \pm \sqrt{\frac{8}{3G}} \frac{v_0^2}{\beta H_0} = \pm 3.0 v_{200}^2 10^{54} \text{ C}, \quad (10)$$

The total EVE/EAE mass corresponds to that of a small galaxy cluster,

$$M = \frac{4v_0^2 R}{3G} = \frac{16}{3\beta\sqrt{6}} \frac{v_0^3}{GH_0} = 2.9 v_{200}^3 10^{13} M_\odot. \quad (11)$$

Assume next that $(5q^2/6R)/(4\pi R^3/3)$, the dark mass density of the cc within R , exceeds ρ_c by a factor $\mu > 1$, while normal matter has the familiar 5% ρ_c . With 25% of mass in ${}^4\text{He}$, the total number of electrons inside R is

$$N_e = \frac{7}{8} \frac{1}{20\mu} \frac{5q^2}{6Rm_N} = \frac{7v_0^3}{48\sqrt{6}\beta\mu GH_0 m_N} = 3.8 v_{200}^3 10^{68}. \quad (12)$$

This is a fraction $5\beta^2/8\mu$ of their cosmic average number, hence $\beta = \sqrt{8\mu/5}$. While all parameters fluctuate from cocoon to cocoon, we take for simplicity $\mu \sim 2.5$, $\beta \sim 2$.

The charge q corresponds to the number of uncompensated electrons within radius r ,

$$\delta N_e(r) = -\frac{q}{e} \frac{r}{R} = -\sqrt{137} \frac{qr}{R} = \mp 8.6 v_{250}^2 10^{55} \frac{r}{R}, \quad (13)$$

so that the charge mismatch ratio results as

$$\delta_e = \frac{\delta N_e(R)}{N_e} = \mp \frac{0.92}{v_{200}} 10^{-13}. \quad (14)$$

While $|\delta_q| \sim 10^{-13}$ is estimated for the solar neighbourhood, values $|\delta_q| \sim 6 \cdot 10^{-15}$ have been reported for $v_{200} = 5$ in the fat galaxy clusters A1689 and A1835 [16].

The typical electric field strength is basically universal,

$$E(r) = \frac{q}{Rr} = \frac{R}{r} \sqrt{\frac{3\mu}{5G}} H_0 \approx 10 \frac{R}{r} \frac{\text{V}}{\text{m}}. \quad (15)$$

The Maxwell equation $\nabla \times \mathbf{B} = \dot{\mathbf{E}}$ sets a typical value

$$B(R) \sim H_0 R E(R) = \frac{H_0 v_{\text{rot}}}{\sqrt{G}} \approx 0.18 v_{200} \mu\text{G}, \quad (16)$$

which connects to the μG scale of cosmic magnetic fields.

A charged cocoon in the expanding Universe.

– As background we consider the Friedman-Lemaître-Robertson-Walker (FLRW) metric with scale factor $a(t)$ and metric $\gamma_{\mu\nu} = \text{diag}(1, -a^2, -a^2 r^2, -a^2 r^2 \sin^2 \theta)$ in spherical coordinates. With energy density ρ_0 and isotropic pressure p_0 , its stress energy tensor takes the form

$$T_0^{\mu\nu} = (\rho_0 + p_0) \delta_0^\mu \delta_0^\nu - p_0 \gamma^{\mu\nu}. \quad (17)$$

The Friedman equations connect them to the scale factor,

$$\rho_0(t) = \frac{3\dot{a}^2}{8\pi G a^2} = \frac{3H^2}{8\pi G}, \quad p_0(t) = -\frac{2a\ddot{a} + \dot{a}^2}{8\pi G a^2}. \quad (18)$$

We shall employ these relations to eliminate ρ_0 and p_0 , so that a cosmological model is not needed yet.

For the temporal development of the cc, we consider the generalized Schwarzschild-FLRW metric

$$\begin{aligned} ds^2 &= g_{\mu\nu} dr^\mu dr^\nu \\ &= g_0 g_1 dt^2 - a^2 \frac{g_0}{g_1} dr^2 - a^2 r^2 g_2 (d\theta^2 + \sin^2\theta d\phi^2), \end{aligned} \quad (19)$$

with $g_i = g_i(t, r)$ and volume element $dV = \sqrt{-g} dr d\theta d\phi$, where $\sqrt{-g} = a^3 g_0 g_2 r^2 \sin\theta$.

The electromagnetic potential and electric field

$$A_\mu = \delta_\mu^0 A_0, \quad E = -A'_0 = \frac{Q(r)}{ar^2}, \quad (20)$$

with $Q(r)$ as in (1), yield the Maxwell stress energy tensor

$$T_{\text{em}\nu}^\mu = \rho_E C_{1\nu}^\mu, \quad C_{1\nu}^\mu = \text{diag}(1, 1, -1, -1), \quad (21)$$

with $\rho_E = Q^2(r)/8\pi a^4 g_0^2 r^4$. The case $g_2(t, r) = g_0(t, r)$ fixes the charge current as $J_q^\nu = F^{\mu\nu}/4\pi = \delta_0^\nu \rho_q(r)/a^3 g_0^2$ and implies the conserved global charge $\int dV J_q^0(t, r) = q$. The electrostatic mass emerges as $M_E(t) = q^2/a(t)R$.

On top of its electrostatic mass, the cocoon can have surplus normal matter of baryons and radiation. While this is often subleading, we include it for generality. Its stress energy tensor is $T_{\text{cc}\nu}^{\mu\nu}(t, r) = T_{\text{cc}\nu}^\mu(t, r)g^{\nu\nu}(t, r)$ with

$$T_{\text{cc}\nu}^\mu = \text{diag}(\rho_{\text{cc}}, -p_{\text{cc}}, -p_{\text{cc}}, -p_{\text{cc}}). \quad (22)$$

Electro-vacuum theory also assumes a vacuum energy density $\rho_\nu(t, r)$ and its radial flux $S_\nu(t, r)$, combined in

$$T_\nu^{\mu\nu} = \rho_\nu g^{\mu\nu} + S_\nu C_{01}^{\mu\nu}, \quad C_{01}^{\mu\nu} = \delta_0^\mu \delta_1^\nu + \delta_1^\mu \delta_0^\nu. \quad (23)$$

The full stress energy tensor contains the background and the cc's material, electrostatic and vacuum terms,

$$T^{\mu\nu} = T_0^{\mu\nu} + T_{\text{cc}}^{\mu\nu} + T_{\text{em}}^{\mu\nu} + T_\nu^{\mu\nu}. \quad (24)$$

We express the Einstein equations as $\bar{G}^\mu_\nu = \bar{T}^\mu_\nu$ where

$$\bar{G}^\mu_\nu \equiv \frac{G^\mu_\nu}{8\pi G} - T_{0\nu}^\mu - T_{\text{cc}\nu}^\mu, \quad \bar{T}^\mu_\nu = T_{\text{em}\nu}^\mu + T_\nu^{\mu\nu}, \quad (25)$$

with lowering of indices by $g_{\mu\nu}$. In the spirit of our earlier approaches, we assume that the FLRW background $T_{0\nu}^\mu$ and the matter component $T_{\text{cc}\nu}^\mu$ are known, so we can express $\bar{\rho}_E \equiv \bar{G}^\mu_\nu C_{1\nu}^\mu/4$ and $\bar{\rho}_\nu \equiv \bar{G}^\mu_\mu/4$ in terms of $g_{0,1}$ and their derivatives. The condition $\bar{G}^0_0 = \bar{G}^1_1$ leads to a quadratic equation for g_1 in terms of g_0 and its derivatives. The results for $\bar{\rho}_E$, $\bar{\rho}_\nu$ and g_1 are given in eqs. (30)–(33) of the Appendix. Taking $S_\nu = G^1_0/8\pi G$ solves the last nontrivial components of the Einstein equations.

Given a cosmological model for $\rho_0(t)$ and $p_0(t)$, and the excess matter profiles $\rho_{\text{cc}}(t, r)$ and $p_{\text{cc}}(t, r)$, the remaining task is to solve $g_0(t, r)$ from $\bar{\rho}_E(t, r) = \rho_E(t, r)$, where

$$\rho_E^{\text{in}} = \frac{q^2}{8\pi a^4 g_0^2 R^2 r^2}, \quad \rho_E^{\text{ex}} = \frac{q^2}{8\pi a^4 g_0^2 r^4}, \quad (26)$$

in the interior and exterior, respectively. Elimination of g_1 leads to a lengthy fourth order partial differential equation for $g_0(t, r)$. From the solution, $\rho_\nu = \bar{\rho}_\nu$ and S_ν can be read off, showing that the vacuum is slaved by electrostatics and matter, as happens in general.

The leading behavior at small r is

$$\bar{\rho}_\nu = \bar{\rho}_E = \frac{1 - g_1(t, 0)}{16\pi G a^2(t) g_0(t, 0) r^2} + \mathcal{O}(r^0). \quad (27)$$

Consistent with (26), it generally has a $1/r^2$ singularity.

Eq. (7) yields $q^2/R^2 = v_0^2/G$ with $v_0 \ll 1$, hence we set

$$g_{0,1}(t, r) = 1 - v_0^2 h_{0,1}(t, r), \quad \rho_{\text{cc}} = v_0^2 \rho_{\text{cc}}^v, \quad p_{\text{cc}} = v_0^2 p_{\text{cc}}^v, \quad (28)$$

and linearize in v_0^2 . The resulting equations are given in eqs. (36)–(38) of the Appendix.

Since $\bar{\rho}_E$ contains the explicit factor $1/r^2$ of ρ_E^{in} of (26), h_0 and h_1 are finite at $r = 0$. We expand

$$h_{0,1}(t, r) = h_{0,1}^{(0)}(t) + h_{0,1}^{(2)}(t)r^2 + h_{0,1}^{(4)}(t)r^4 + \dots \quad (29)$$

At $r = 0$, the condition $\bar{\rho}_E/\rho_E^{\text{in}} = 1$ yields $h_1^{(0)} = 2/a^2$. Given a shape for $h_0^{(0)}(t)$, the expression (38) for h_1 then yields $h_0^{(2)}(t)$. Likewise, order r^2 will set $h_0^{(4)}(t)$, and so on. This provides a proper boundary condition for numerical integration from small r up to R .

At large r , the Ansatz $h_0 \approx k_4(t)/r^4 + k_6(t)/r^6$, $h_1 \approx l_4(t)/r^4 + l_6(t)/r^6$ solves l_4 in terms of k_4 , \dot{k}_4 and \ddot{k}_4 , so that $\bar{\rho}_E/\rho_E^{\text{ex}} = 1$ leads to a fourth order differential equation for $k_4(t)$ in terms of $a(t)$ and possibly $\sigma_4(t)$ and $\tau_4(t)$ from the asymptotics $\rho_{\text{cc}}^v \approx \sigma_4/r^4 + \sigma_6/r^6$, $p_{\text{cc}}^v \approx \tau_6/r^4 + \tau_6/r^6$. Next order determines $k_6(t)$. One can thus solve h_0 from large r down to R and equate $h_0(t, R^+)$ to $h_0(t, R^-)$ by adjusting $h_0^{(0)}(t)$. Hence the problem is uniquely posed, also beyond linearity. The resulting decay $S_\nu \sim 1/r^5$ confirms that no vacuum energy flows in from infinity into the cocoon.

Fit in the early Universe. The above analysis affirms that the cocoons have comoving size $R \sim 2$ Mpc. The comoving horizon passes R for $z \sim 2.3 \cdot 10^5$ or $T \sim 55$ eV; at higher z the cocoon is only partly in causal contact.

With Planck redshift $z_P = \sqrt{1/G}/2.725 \text{ K} = 5.2 \cdot 10^{31}$, the ccs have physical radius $R_P = R/z_P \sim 1.2$ nm at the Big Bang. The average charge per Planck volume $q(\ell_P/R_P)^3 \sim 8.8 \cdot 10^{-23} e$ may relate to a unit of mini-charge. We recall that in the Lorentz model for the electron, its charge stems from a shell of discrete or continuous mini-charges [17, 18, 20].

Discussion. – Recently, Mistele et al. [4] analyze the weak lensing of isolated galaxies. The observations imply “indefinite flattening of rotation curves”, viz. the constancy of circular rotation speeds persists up to distances of 1 Mpc, the size of galaxy clusters. This size of dark matter “cocoons” is much larger than expected from Λ CDM, and difficult to explain within this theory.

The situation is modeled as “charged cocoons” within our recent electro-vacuum theory; the latter applies to

vastly different scales from the Lorentz electron [17] to black holes [15] and the whole cosmos [16]. In this theory, dark matter does not stem from some unknown particle but is a combination of electrostatic and vacuum energy, with the Coulomb repulsion of like charges stabilized by the Poincaré stress (negative pressure) of the vacuum. For the cocoons, a $\pm 1/r^2$ charge density profile leads to a rotation profile that is basically flat up to 1 Mpc. The dark mass of the cocoon coincides with the typical mass of a small galaxy cluster. Different shapes of the charge profile can be considered.

On the Mpc scale, the enclosed mass components occur at their cosmic fractions, so that the indirectly observed circular rotation speeds $v \sim 200$ km/s confirm the typical cocoon radius $R \sim v/H_0 \sim 2$ Mpc.

Like most galaxies, those with a charged cocoon likely contain a central supermassive black hole. Black holes created by stellar collapse inside charged cocoons are naturally charged. Indeed, the cocoon's charge-to-mass ratio $q/M\sqrt{G} \sim c/v_0 \sim 1500$ for $v_0 \sim 200$ km/s, is much larger than the value 1 of an extremal black hole. This supports physical realization of our exact solutions for non-rotating, charged black holes with a regular core [15].

The cocoon size and mass, being comparable to that of galaxy clusters, hints at a common nature. In this view, clusters involve several plus and minus charged cocoons. As mentioned below (14), the charge mismatch factor δ_e in the solar neighborhood matches the estimates from ccs. The smaller values in the fat clusters A1689 and A1835 may express a mixture of such cocoons of either charge. In between the clusters, there may be many charged cocoons.

The present-day analytical solution is generalized to the expanding Universe and expressed in a partial differential equation involving the FLRW background.

That the charged cocoons arise from merging of smaller ones is unlikely, if only because these must mainly have the same sign of their net charges on the comoving Mpc scale. If they neither arise from an instability, they must be present at the Big Bang, with nanometer size in the Planck regime. The involved inhomogeneous initial state offers a new starting point for the study of the baryon asymmetry and the ${}^7\text{Li}$ problem. In fact, the 1.2 nm physical cocoon size at the Big Bang equals $\exp(60)$ Planck lengths $\ell_P = \sqrt{G}$, so that after 60 e -folds the inhomogeneous initial state becomes homogeneous. This may be related to the 60 e -folds expected for a graceful exit of inflation [21].

The “little red dots”, compact and extremely red galaxies at $z \geq 4$ [22], may exhibit a similar connection to ccs.

The existence of Mpc sized cocoons predicts a peak in the cosmic microwave background at the arcmin scale or angular index $l \sim 8000$. Both the South Pole Telescope [23] (data up to $l = 5000$) and the Atacama Cosmology Telescope [24] (data up to $l = 7500$) observe an upward trend in the temperature spectrum for $l \gtrsim 3000$. While this has been explained in terms of cosmic foregrounds, it is interesting to test a connection to cocoons, and to

extend the observations towards the arcsec regime.

Finally one may speculate about the origin of the induced nanometer sized cocoons at the Big Bang. For instance, the collapse of the Universe in a previous aeon after all matter and remaining energy ended up in supermassive black holes, a case connecting to a cyclic Universe.

REFERENCES

- [1] ZWICKY F., *Helvetica Physica Acta*, **6** (1933) 110.
- [2] RUBIN V. C. and FORD JR W. K., *The Astrophysical Journal*, **159** (1970) 379.
- [3] RUBIN V. C., FORD JR W. K. and THONNARD N., *Astrophysical Journal, Part 1, vol. 238, June 1, 1980, p. 471-487.*, **238** (1980) 471.
- [4] MISTELE T., MCGAUGH S., LELLI F., SCHOMBERT J. and LI P., *The Astrophysical Journal Letters*, **969** (2024) L3.
- [5] NAVARRO J. F., FRENK C. S. and WHITE S. D., *The Astrophysical Journal*, **490** (1997) 493.
- [6] MILGROM M., *The Astrophysical Journal*, **270** (1983) 365.
- [7] BANIK I. and ZHAO H., *Symmetry*, **14** (2022) 1331.
- [8] VERLINDE E., *Journal of High Energy Physics*, **2011** (2011) 1.
- [9] VERLINDE E., *SciPost Physics*, **2** (2017) 016.
- [10] BANIK I., PITTORDIS C., SUTHERLAND W., FAMAEE B., IBATA R., MIESKE S. and ZHAO H., *Monthly Notices of the Royal Astronomical Society*, **527** (2024) 4573.
- [11] HERNANDEZ X., CHAE K.-H. and AGUAYO-ORTIZ A., *Monthly Notices of the Royal Astronomical Society*, **533** (2024) 729.
- [12] SANDERS R., *Monthly Notices of the Royal Astronomical Society*, **342** (2003) 901.
- [13] NIEUWENHUIZEN T. M., *Fortschritte der Physik*, **65** (2017) 1600050.
- [14] DESMOND H., HEES A. and FAMAEE B., *Monthly Notices of the Royal Astronomical Society*, **530** (2024) 1781.
- [15] NIEUWENHUIZEN T. M., *arXiv preprint arXiv:2302.14653*, (2023) .
- [16] NIEUWENHUIZEN T. M., *Frontiers in Astronomy and Space Sciences*, **11** (2024) 1413816.
- [17] NIEUWENHUIZEN T. M., *submitted*, (2024) .
- [18] POINCARÉ H., *Comptes Rendus hebdomadaires des séances de l'Académie des Sciences et belles-lettres*, **140** (1905) 1504.
- [19] DAMOUR T., *Comptes Rendus Physique*, **18** (2017) 551.
- [20] LORENTZ H. A., *Physikalische Zeitschrift*, **2** (1901) 78.
- [21] LIDDLE A. R. and LYTH D. H., *Cosmological inflation and large-scale structure* (Cambridge university press) 2000.
- [22] AKINS H. B., CASEY C. M., LAMBRIDES E., ALLEN N., ANDIKA I. T., BRINCH M., CHAMPAGNE J. B., COOPER O., DING X., DRAKOS N. E. ET AL., *arXiv preprint arXiv:2406.10341*, (2024) .
- [23] HENNING J., SAYRE J., REICHARDT C., ADE P., ANDERSON A., AUSTERMANN J., BEALL J., BENDER A., BENSON B., BLEEM L. ET AL., *The Astrophysical Journal*, **852** (2018) 97.
- [24] CHOI S. K., HASSELFIELD M., HO S.-P. P., KOOPMAN B., LUNGU M., ABITBOL M. H., ADDISON G. E., ADE P. A., AIOLA S., ALONSO D. ET AL., *Journal of Cosmology and Astroparticle Physics*, **2020** (2020) 045.

Appendix. – The expression for $\bar{\rho}_v(t, r)$ in terms of $a(t)$, $g_{0,1}(t, r)$, and $\rho_{cc}(t, r)$ and $p_{cc}(t, r)$ reads

$$\begin{aligned} \bar{\rho}_v = & \frac{1}{8\pi G} \left[\frac{1-g_0g_1}{2a^2g_0r^2} - \frac{g_1'}{a^2g_0r} - \frac{3g_0'g_1}{2a^2g_0^2r} + \frac{\dot{a}^2}{4a^2} \left(\frac{6}{g_0g_1} - 2g_0 - \frac{g_0}{g_1} - 3g_0g_1 \right) - \frac{3g_0''g_1}{4a^2g_0^2} + \frac{3g_0'^2g_1}{8a^2g_0^3} - \frac{3g_0'g_1'}{4a^2g_0^2} - \frac{g_1''}{4a^2g_0} \right. \\ & \left. + \frac{\ddot{a}}{2a} \left(\frac{3}{g_0g_1} - 2g_0 - \frac{g_0}{g_1} \right) + \frac{\dot{a}}{a} \frac{9\dot{g}_0g_1 - 7g_0\dot{g}_1}{4g_0^2g_1^2} + \frac{3\ddot{g}_0}{4g_0^2g_1} - \frac{\dot{g}_1}{4g_0g_1^2} - \frac{3\dot{g}_0^2}{8g_0^3g_1} - \frac{3\dot{g}_0\dot{g}_1}{4g_0^2g_1^2} + \frac{\dot{g}_1^2}{2g_0g_1^3} \right] - \frac{\rho_{cc} - 3p_{cc}}{4}. \end{aligned} \quad (30)$$

Likewise, the expression for $\bar{\rho}_E$ reads

$$\begin{aligned} \bar{\rho}_E = & \frac{1}{8\pi G} \left[\frac{1-g_0g_1}{2a^2g_0r^2} - \frac{g_0'g_1}{2a^2g_0^2r} + \frac{\dot{a}^2}{4a^2} \left(2g_0 - \frac{g_0}{g_1} + \frac{2}{g_0g_1} - 3g_0g_1 \right) + \frac{1}{4a^2g_0} \left(\frac{g_0''g_1}{g_0} - \frac{3g_0'^2g_1}{2g_0^2} + \frac{g_0'g_1'}{g_0} + g_1'' \right) \right. \\ & \left. + \frac{\ddot{a}}{a} \left(g_0 - \frac{g_0}{2g_1} - \frac{1}{2g_0g_1} \right) + \frac{3\dot{a}\dot{g}_1}{4ag_0g_1^2} + \frac{\dot{a}\dot{g}_0}{4ag_0^2g_1} - \frac{\ddot{g}_0}{4g_0^2g_1} + \frac{\ddot{g}_1}{4g_0g_1^2} + \frac{3\dot{g}_0^2}{8g_0^3g_1} + \frac{\dot{g}_0\dot{g}_1}{4g_0^2g_1^2} - \frac{\dot{g}_1^2}{2g_0g_1^3} \right] - \frac{\rho_{cc} + p_{cc}}{4}. \end{aligned} \quad (31)$$

The solution for g_1 reads

$$g_1 = \frac{\sqrt{g_w} - 8\pi G(\rho_{cc} + p_{cc})a^2g_0^3}{g_0(6\dot{a}^2g_0^4 + 2g_0''g_0 - 3g_0'^2)}, \quad (32)$$

with

$$\begin{aligned} g_w = & 2\dot{a}^2(g_0^2 + 2)g_0^2(6\dot{a}^2g_0^4 + 2g_0''g_0 - 3g_0'^2) + a^2(2\ddot{g}_0g_0 - 3\dot{g}_0^2)[3g_0'^2 - 2g_0(3\dot{a}^2g_0^3 + g_0'')] \\ & + 2ag_0[2\ddot{a}g_0(g_0^2 - 1) + \dot{a}\dot{g}_0](6\dot{a}^2g_0^4 + 2g_0''g_0 - 3g_0'^2) + [8\pi G(\rho_{cc} + p_{cc})a^2g_0^3]^2. \end{aligned} \quad (33)$$

In the interior one has to solve $g_{0,1}(t, r)$ from $\bar{\rho}_E = \rho_E^{\text{in}}$ and in the exterior from $\bar{\rho}_E = \rho_E^{\text{ex}}$, where

$$\rho_E^{\text{in}} = \frac{v_0^2}{8\pi G a^4 g_0^2 r^2}, \quad \rho_E^{\text{ex}} = \frac{v_0^2 R^2}{8\pi G a^4 g_0^2 r^4}. \quad (34)$$

The expansion up to order v_0^2 ,

$$g_0(t, r) = 1 - v_0^2 h_0(t, r), \quad g_1(t, r) = 1 - v_0^2 h_1(t, r), \quad \rho_{cc}(t, r) = v_0^2 \rho_{cc}^v(t, r), \quad p_{cc}(t, r) = v_0^2 p_{cc}^v(t, r), \quad (35)$$

yields the linearized expressions

$$\bar{\rho}_v = \frac{v_0^2}{8\pi G} \left[\frac{h_1}{2a^2r^2} + \frac{3h_0' + 2h_1'}{2a^2r} + \frac{3h_0'' + h_1''}{4a^2} - \frac{3\ddot{h}_0 - \ddot{h}_1}{4} + \frac{\ddot{a}}{a}(3h_0 + h_1) + \frac{\dot{a}^2}{a^2}(3h_0 + 2h_1) - \frac{\dot{a}}{a} \frac{9\dot{h}_0 - 7\dot{h}_1}{4} \right] - v_0^2 \frac{\rho_{cc}^v - 3p_{cc}^v}{4}, \quad (36)$$

and

$$\bar{\rho}_E = \frac{v_0^2}{8\pi G} \left[\frac{h_1}{2a^2r^2} + \frac{h_0'}{2a^2r} - \frac{h_0'' + h_1''}{4a^2} + \frac{\ddot{h}_0 - \ddot{h}_1}{4} - \frac{\ddot{a}}{a}(h_0 + h_1) + \frac{\dot{a}^2}{a^2}(h_0 + h_1) - \frac{\dot{a}}{a} \frac{\dot{h}_0 + 3\dot{h}_1}{4} \right] - v_0^2 \frac{\rho_{cc}^v + p_{cc}^v}{4}. \quad (37)$$

The linearized version of (32), (33) reads

$$h_1 = -\frac{a^2}{6\dot{a}^2}\ddot{h}_0 + \frac{2a\ddot{a}}{3\dot{a}^2}h_0 + \frac{a}{6\dot{a}}\dot{h}_0 - \frac{2}{3}h_0 - \frac{h_0''}{6\dot{a}^2} + \frac{a^2}{6\dot{a}^2}(\rho_{cc}^v + p_{cc}^v). \quad (38)$$

To order v_0^2 , eq. (34) reduces to

$$\rho_E^{\text{in}} = \frac{v_0^2}{8\pi G a^4 r^2}, \quad \rho_E^{\text{ex}} = \frac{v_0^2 R^2}{8\pi G a^4 r^4}. \quad (39)$$